

A common behavior of thermoelectric layered cobaltites: incommensurate spin density wave states in [Ca₂Co_{4/3}Cu_{2/3}O₄]_{0.62}[CoO₂] and [Ca₂CoO₃]_{0.62}[CoO₂]

J Sugiyama^{†§}, J H Brewer[‡], E J Ansaldo^{||}, H Itahara[†], K Dohmae[†], C Xia[†], Y Seno[†], B Hitti^{||} and T Tani[†]

[†] Toyota Central Research and Development Labs. Inc., Nagakute, Aichi 480-1192, Japan

[‡] TRIUMF, CIAR and Department of Physics and Astronomy, University of British Columbia, Vancouver, BC, V6T 1Z1 Canada

^{||} TRIUMF, 4004 Wesbrook Mall, Vancouver, BC, V6T 2A3 Canada

Abstract. Magnetism of a misfit layered cobaltite [Ca₂Co_{4/3}Cu_{2/3}O₄]_x^{RS}[CoO₂] ($x \sim 0.62$, RS denotes a rocksalt-type block) was investigated by a positive muon spin rotation and relaxation (μ^+ SR) experiment. A transition to an incommensurate (IC) spin density wave (SDW) state was found below 180 K ($= T_C^{\text{on}}$); and a clear oscillation due to a static internal magnetic field was observed below 140 K ($= T_C$). Furthermore, an anisotropic behavior of the zero-field μ^+ SR experiment indicated that the IC-SDW propagates in the a - b plane, with oscillating moments directed along the c axis. These results were quite similar to those for the related compound [Ca₂CoO₃]_{0.62}^{RS}[CoO₂], *i.e.*, Ca₃Co₄O₉. Since the IC-SDW field in [Ca₂Co_{4/3}Cu_{2/3}O₄]_{0.62}^{RS}[CoO₂] was approximately same to those in pure and doped [Ca₂CoO₃]_{0.62}^{RS}[CoO₂], it was concluded that the IC-SDW exist in the [CoO₂] planes.

PACS numbers: 76.75.+i, 75.30.Fv, 75.50.Gg, 72.15.Jf

§ To whom correspondence should be addressed.

1. Introduction

Layered cobaltites are investigated eagerly because of their structural and compositional variety and also their good thermoelectric properties. At present, the following three groups of cobaltites are known to be good thermoelectrics, because they display metallic conductivities as well as high thermoelectric powers S , for reasons which are currently not fully understood. A sodium cobaltite, Na_xCoO_2 , was the first compound reported as a good thermoelectric material [1, 2, 3]. Then, the finding of $[\text{Ca}_2\text{CoO}_3]_{0.62}^{\text{RS}}[\text{CoO}_2]$ [4, 5, 6], and then $[\text{Sr}_2\text{Bi}_{2-y}\text{Pb}_y\text{O}_4]_x^{\text{RS}}[\text{CoO}_2]$ [7, 8, 9], followed [14], where RS denotes a rocksalt-type block. All share a common structural component, the CoO_2 planes, in which a two-dimensional-triangular lattice of Co ions is formed by a network of edge-sharing CoO_6 octahedra. Charge carrier transport in these cobaltites is thought to be restricted mainly to the CoO_2 planes, as in the case of the CuO_2 planes for the high- T_c cuprates.

Recent positive muon spin rotation and relaxation ($\mu^+\text{SR}$) experiments on $[\text{Ca}_2\text{CoO}_3]_{0.62}^{\text{RS}}[\text{CoO}_2]$ [10, 11, 12, 13] indicated the existence of an incommensurate (IC) spin density wave (SDW) state below 100 K, which was not detected previously by other magnetic measurements [5, 6, 10]. The latter two experiments suggested that a long-range IC-SDW order completed below ~ 30 K, while a short-range order appeared below 100 K [12, 13]. Since the $\rho(T)$ curve exhibits a broad minimum around 80 K [5, 6, 10], the behavior of conduction electrons is found to be strongly affected even by their short-range magnetic order.

A new thermoelectric layered cobaltite $[\text{Ca}_2\text{Co}_{4/3}\text{Cu}_{2/3}\text{O}_4]_{0.62}^{\text{RS}}[\text{CoO}_2]$ was found recently [14]; the crystal structure consists of alternating layers of the quadruple rocksalt-type $[\text{Ca}_2\text{Co}_{4/3}\text{Cu}_{2/3}\text{O}_4]$ subsystem and the single CdI_2 -type $[\text{CoO}_2]$ subsystem stacked along the c axis. There is a misfit between these subsystems along the b -axis, similar to the case of $[\text{Ca}_2\text{CoO}_3]_{0.62}^{\text{RS}}[\text{CoO}_2]$ [5, 6]. Polycrystalline $[\text{Ca}_2\text{Co}_{4/3}\text{Cu}_{2/3}\text{O}_4]_{0.62}^{\text{RS}}[\text{CoO}_2]$ samples have values of thermopower $S = 150 \mu\text{VK}^{-1}$ and resistivity $\rho = 15 \text{ m}\Omega\text{cm}$ at 300 K [14]. As a result, their thermoelectric power factor ($= S^2\rho^{-1}$) is $\sim 20\%$ larger than that of polycrystalline $[\text{Ca}_2\text{CoO}_3]_{0.62}^{\text{RS}}[\text{CoO}_2]$ samples. Since the $\rho(T)$ curve exhibited a broad minimum and the $S(T)$ curve a broad maximum around 130 K, there seems to exist a transition from a high-temperature metallic to a low-temperature insulator state around 130 K. On the other hand, susceptibility (χ) measurements indicate no anomalies around 130 K, although χ showed a small change at ~ 80 K.

Therefore, $\mu^+\text{SR}$ experiments on $[\text{Ca}_2\text{Co}_{4/3}\text{Cu}_{2/3}\text{O}_4]_{0.62}^{\text{RS}}[\text{CoO}_2]$ are also expected to provide crucial information on the correlation between magnetism and transport properties in the layered cobaltites. Furthermore, such experiment is significant to clarify the universal behavior of magnetism in thermoelectric layered cobaltites. Here, we report both weak (~ 100 Oe) transverse-field (wTF-) $\mu^+\text{SR}$ and zero field (ZF-) $\mu^+\text{SR}$ measurements for a c axis aligned $[\text{Ca}_2\text{Co}_{4/3}\text{Cu}_{2/3}\text{O}_4]_{0.62}^{\text{RS}}[\text{CoO}_2]$ sample at temperatures below 300 K. The former method is sensitive to local magnetic order *via* the shift of the μ^+ spin precession frequency and the enhanced μ^+ spin relaxation, while ZF-

μ^+ SR is sensitive to weak local magnetic [dis]order in samples exhibiting quasi-static paramagnetic moments.

2. Experiment

A c -axis aligned polycrystalline $[\text{Ca}_2\text{Co}_{4/3}\text{Cu}_{2/3}\text{O}_4]_{0.62}^{\text{RS}}[\text{CoO}_2]$ plate ($\sim 15 \times 10 \times 2 \text{ mm}^3$) was synthesized by a reactive templated grain growth technique [15]. In addition, c -axis aligned cobaltites with the triple rocksalt-type subsystem, *i.e.*, $[\text{Ca}_2\text{CoO}_3]_{0.62}^{\text{RS}}[\text{CoO}_2]$ and $[\text{Ca}_{1.8}\text{M}_{0.2}\text{CoO}_3]_x^{\text{RS}}[\text{CoO}_2]$ ($M = \text{Sr}, \text{Y}$ and Bi) plates were prepared for comparison. Then, the c -aligned plates were annealed at 450 °C for 12 hours in an oxygen flow. Powder X-ray diffraction (XRD) studies indicated that all the samples were single phase with a monoclinic structure and almost 100% aligned along the c axis. The preparation and characterization of these samples were described in detail elsewhere [16].

Magnetic susceptibility (χ) was measured using a superconducting quantum interference device (SQUID) magnetometer (mpms, *Quantum Design*) in a magnetic field of less than 55 kOe. The μ^+ SR experiments were performed on the **M15** or **M20** surface muon beam lines at TRIUMF. The experimental setup and techniques are described elsewhere [17].

3. Results

3.1. $[\text{Ca}_2\text{Co}_{4/3}\text{Cu}_{2/3}\text{O}_4]_{0.62}^{\text{RS}}[\text{CoO}_2]$

Figures 1(a) and 1(b) show the temperature dependences of χ and χ^{-1} for the c -aligned $[\text{Ca}_2\text{Co}_{4/3}\text{Cu}_{2/3}\text{O}_4]_{0.62}^{\text{RS}}[\text{CoO}_2]$ sample. In order to determine anisotropy, the magnetic field H was applied parallel or perpendicular to the ab plane. Hereby, we abbreviate χ obtained with $H \perp ab$ as χ_c and $H // ab$ as χ_{ab} , respectively. The $\chi_c(T)$ curve in a zero-field cooling (ZFC) mode exhibits a cusp at $\sim 85 \text{ K}$; also, a clear thermal hysteresis is seen between the data obtained in a ZFC mode and a field cooling (FC) mode. On the other hand, as T decreases, χ_{ab}^{-1} decreases monotonically with increasing slope ($d\chi_{ab}^{-1}/dT$), although there is a small anomaly at $\sim 85 \text{ K}$, probably due to a misalignment between the sample axis and H . Nevertheless, the magnetization (M) – H curve did not show a clear loop even at 5 K. These results suggest that $[\text{Ca}_2\text{Co}_{4/3}\text{Cu}_{2/3}\text{O}_4]_{0.62}^{\text{RS}}[\text{CoO}_2]$ undergoes a magnetic transition to either a ferrimagnetic or a spin glass state at 80 K with the easiest magnetization direction parallel to the c -axis. It is worth noting that there are no marked anomalies in Figure 1 except for the cusp in the $\chi_c(T)$ at $\sim 85 \text{ K}$.

The wTF- μ^+ SR spectra in a magnetic field of $H \sim 100 \text{ Oe}$ in the c -aligned $[\text{Ca}_2\text{Co}_{4/3}\text{Cu}_{2/3}\text{O}_4]_{0.62}^{\text{RS}}[\text{CoO}_2]$ sample exhibit a clear reduction of the μ^+ precession amplitude below 200 K. The wTF- μ^+ SR spectrum below 200 K was well fitted in the time domain with a combination of a slowly relaxing precessing signal and two non-oscillatory signals, one fast and the other slow relaxing:

$$A_0 P(t) = A_{\text{para}} \exp(-\lambda_{\text{para}} t) \cos(\omega_{\mu} t + \phi)$$

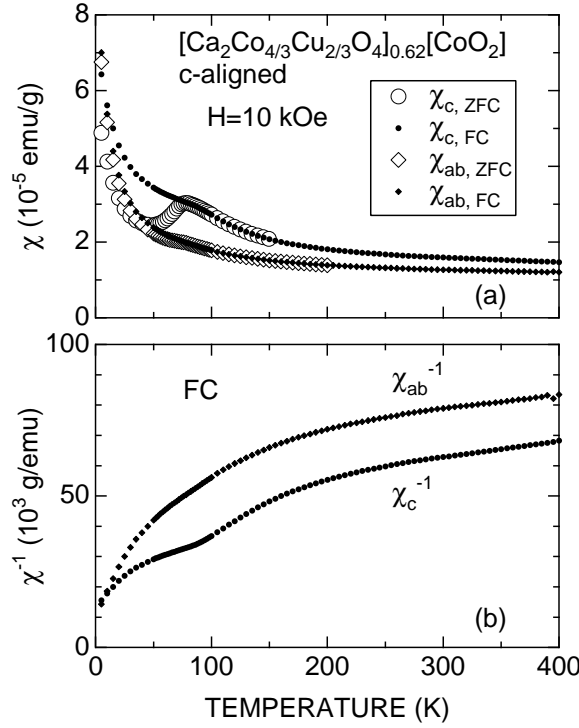


Figure 1. Temperature dependences of (a) susceptibility χ and (b) χ^{-1} for c -aligned $[\text{Ca}_2\text{Co}_{4/3}\text{Cu}_{2/3}\text{O}_4]_{0.62}^{\text{RS}}[\text{CoO}_2]$.

$$\begin{aligned}
 &+ A_{\text{fast}} \exp(-\lambda_{\text{fast}} t) \\
 &+ A_{\text{slow}} \exp(-\lambda_{\text{slow}} t),
 \end{aligned} \tag{1}$$

where A_0 is the initial asymmetry, $P(t)$ is the muon spin polarization function, ω_μ is the muon Larmor frequency, ϕ is the initial phase of the precession and A_n and λ_n ($n = \text{para, fast and slow}$) are the asymmetries and exponential relaxation rates of the three signals. The latter two signals ($n = \text{fast and slow}$) have finite amplitudes below ~ 180 K.

Figures 2(a) - 2(d) show the temperature dependences of A_{para} , λ_{para} , A_n ($n = \text{fast and slow}$) and λ_n in the c -aligned $[\text{Ca}_2\text{Co}_{4/3}\text{Cu}_{2/3}\text{O}_4]_{0.62}^{\text{RS}}[\text{CoO}_2]$ sample. The large decrease in A_{para} below 180 K (and the accompanying increase in λ_{para}) indicate the existence of a magnetic transition with an onset temperature $T_c^{\text{on}} \sim 180$ K, a transition width $\Delta T \sim 40$ K and an endpoint $T_c^{\text{end}} \sim 140$ K, respectively. Since A_{para} is roughly proportional to the volume of a paramagnetic phase, this result ($A_{\text{para}} \sim 0$ below T_c^{end}) suggests that almost all the sample changes into a magnetically ordered state below 140 K.

Figure 3 shows ZF- μ^+ SR time spectra at 2.1 K in the c -aligned sample; the top spectrum was obtained with the initial μ^+ spin direction $\vec{S}_\mu(0)$ perpendicular to the c -axis and the bottom one with $\vec{S}_\mu(0) \parallel c$. A clear oscillation due to quasi-static internal fields is observed only when $\vec{S}_\mu(0) \perp c$. This oscillating spectrum is reasonably well fitted with a combination of two zeroth-order Bessel functions of the first kind J_0 (for

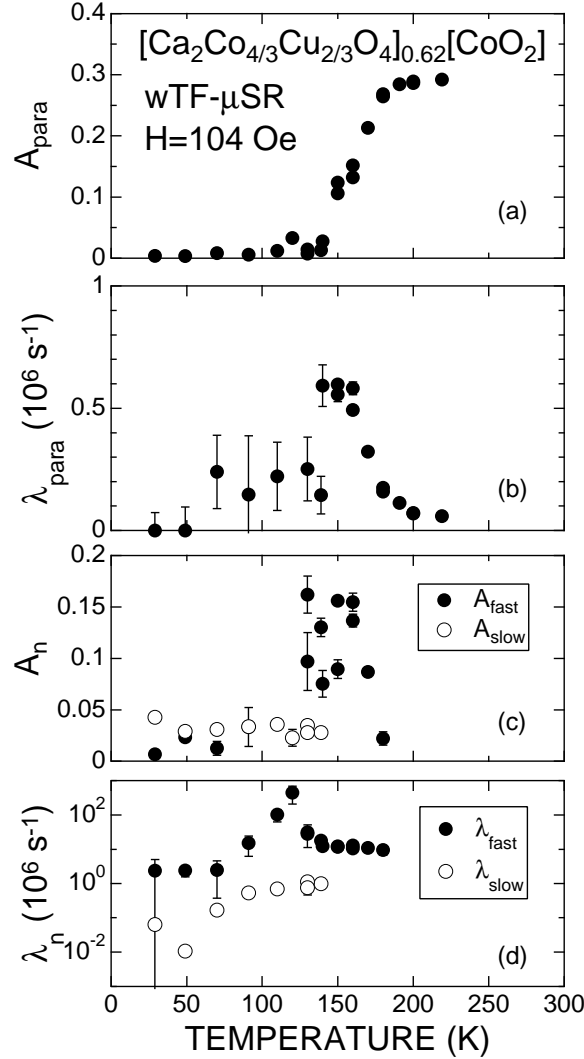


Figure 2. Temperature dependences of (a) A_{para} , (b) λ_{para} , (c) A_n and (d) λ_n ($n = \text{fast and slow}$) in c -aligned $[\text{Ca}_2\text{Co}_{4/3}\text{Cu}_{2/3}\text{O}_4]_{0.62}^{\text{RS}}[\text{CoO}_2]$. The data were obtained by fitting the wTF- μ^+ SR spectra using equation (1).

the IC-SDW)[17, 18, 19] and an exponential relaxation function:

$$\begin{aligned}
 A_0 P(t) = & A_{\text{SDW1}} J_0(\omega_\mu t) \exp(-\lambda_{\text{SDW1}} t) \\
 & + A_{\text{SDW2}} J_0(\omega_\mu t) \exp(-\lambda_{\text{SDW2}} t) \\
 & + A_{\text{F}} \exp(-\lambda_{\text{F}} t)
 \end{aligned} \tag{2}$$

$$\omega_\mu \equiv 2\pi\nu_\mu = \gamma_\mu H_{\text{int}} \tag{3}$$

where A_0 is the empirical maximum muon decay asymmetry, A_{SDW1} , A_{SDW2} and A_{F} are the asymmetries and λ_{SDW1} , λ_{SDW2} and λ_1 are the exponential relaxation rates associated with the three signals. Also, ω_μ is the muon precession frequency in the characteristic local magnetic field H_{int} due to an IC-SDW and γ_μ is muon gyromagnetic ratio. The two Bessel functions in equation (2) indicate that there are two inequivalent muon sites

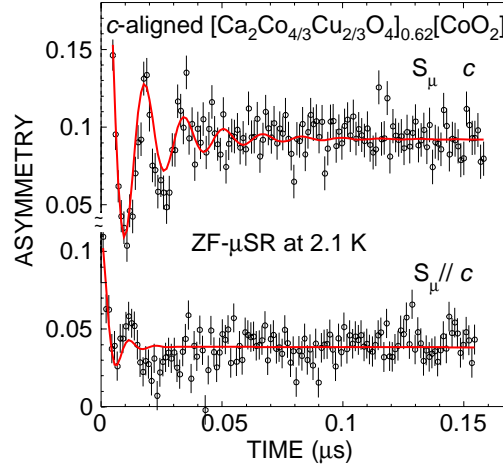


Figure 3. ZF- μ^+ SR time spectra of the c -aligned $[\text{Ca}_2\text{Co}_{4/3}\text{Cu}_{2/3}\text{O}_4]_{0.62}^{\text{RS}}[\text{CoO}_2]$ plate at 2.1 K. The configurations of the sample and the muon beam are (top) $\vec{S}_\mu(0) \perp c$ and (bottom) $\vec{S}_\mu(0) \parallel c$, where $\vec{S}_\mu(0)$ indicates the initial muon spin direction.

in the $[\text{Ca}_2\text{Co}_{4/3}\text{Cu}_{2/3}\text{O}_4]_{0.62}^{\text{RS}}[\text{CoO}_2]$ lattice, because the three signals have a finite value below 140 K. Due to some broadening of the IC-SDW field distribution, the two Bessel functions exhibit an exponential damping.

We therefore conclude that $[\text{Ca}_2\text{Co}_{4/3}\text{Cu}_{2/3}\text{O}_4]_{0.62}^{\text{RS}}[\text{CoO}_2]$ undergoes a magnetic transition from a paramagnetic state to an IC-SDW state, similar to the case of $[\text{Ca}_2\text{CoO}_3]_{0.62}^{\text{RS}}[\text{CoO}_2]$. [10, 11, 13] The absence of a clear oscillation in the bottom spectrum of Figure 3 indicates that the internal magnetic field \vec{H}_{int} is roughly parallel to the c axis [13], since the muon spins do not precess in a parallel magnetic field. The IC-SDW is unlikely to propagate along the c axis due both to the two-dimensionality and to the misfit between the two subsystems. The IC-SDW is therefore considered to propagate in the a - b plane, with oscillating moments directed along the c axis.

In the $[\text{Ca}_2\text{Co}_{4/3}\text{Cu}_{2/3}\text{O}_4]$ subsystem, 1/3 of the Co sites are randomly substituted by Cu [14]. This means that 2 or 3 of the eight of the first nearest neighboring Co ions are replaced by Cu for each Co ion in the $[\text{Ca}_2\text{Co}_{4/3}\text{Cu}_{2/3}\text{O}_4]$ subsystem. Nevertheless, a clear precession was observed in the ZF- μ^+ SR spectrum below 140 K. In addition, the precession frequency (~ 60 MHz) at zero temperature is almost the same as to $[\text{Ca}_2\text{CoO}_3]_{0.62}^{\text{RS}}[\text{CoO}_2]$ (~ 56 MHz). Since the long-range order of the Co moments in the $[\text{Ca}_2\text{Co}_{4/3}\text{Cu}_{2/3}\text{O}_4]$ subsystem should be strongly hindered by Cu, it is concluded that the IC-SDW exists not in the $[\text{Ca}_2\text{Co}_{4/3}\text{Cu}_{2/3}\text{O}_4]$ subsystem but in the $[\text{CoO}_2]$ plane.

Figures 4(a) - 4(c) show the temperature dependences of A_n ($n = \text{SDW1, SDW2}$ and F), $\nu_{\mu n}$ ($n = 1$ and 2) and λ_n ($n = \text{SDW1, SDW2}$ and F). It is clearly seen that the signal associated with the SDW1 is the predominant one among the three signals. The volume fraction of the signal from the SDW1 is estimated as $\sim 100\%$ at 2.1 K. This suggests that almost all the μ^+ are bound to the oxygen ions in the $[\text{CoO}_2]$ plane, with only at the very small portion in the $[\text{Ca}_2\text{Co}_{4/3}\text{Cu}_{2/3}\text{O}_4]$ subsystem. Therefore, we

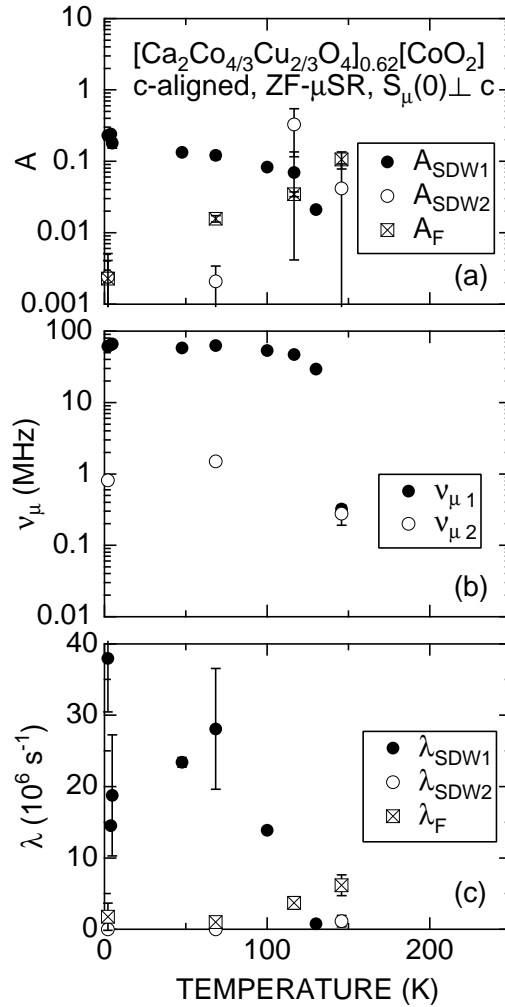


Figure 4. Temperature dependences of (a) A_n ($n = \text{SDW1}$, SDW2 and F), (b) $\nu_{\mu n}$ ($n = 1$ and 2) and (c) λ_n ($n = \text{SDW1}$, SDW2 and F) for the c -aligned $[\text{Ca}_2\text{Co}_{4/3}\text{Cu}_{2/3}\text{O}_4]_{0.62}^{\text{RS}}[\text{CoO}_2]$. The data was obtained by fitting of the ZF- μ^+ SR time spectra using equation (2).

consider the signal of the **SDW1** and ignore the contribution from the other signals.

Figures 5(a) - 5(d) show the temperature dependences of A_{SDW1} , $\nu_{\mu 1}$, λ_{SDW1} , and in-plane resistivity (ρ_{ab}). In particular, A_{SDW1} increases monotonically with decreasing T from 140 K, although A_{para} obtained by the wTF- μ^+ SR measurement exhibits a rapid decrease below 200 K and levels off to almost 0 below 140 K (see Figure 5(a)). This suggests that a long-range IC-SDW order completes below ~ 140 K ($= T_{\text{SDW}}$), while a short-range order appears below 200 K ($= T_{\text{SDW}}^{\text{on}}$), as in the case of $[\text{Ca}_2\text{CoO}_3]_{0.62}^{\text{RS}}[\text{CoO}_2]$ [12, 13]. Actually, this is in good agreement with the temperature dependence of ρ_{ab} ; that is, $\rho_{ab}(T)$ is metallic above 140 K and semiconducting below 140 K. On the other hand, there was no clear anomalies around 140 K in the $\chi(T)$ curve (see Fig. 1) probably due to effects of the grain boundaries, a possible inhomogeneous distribution

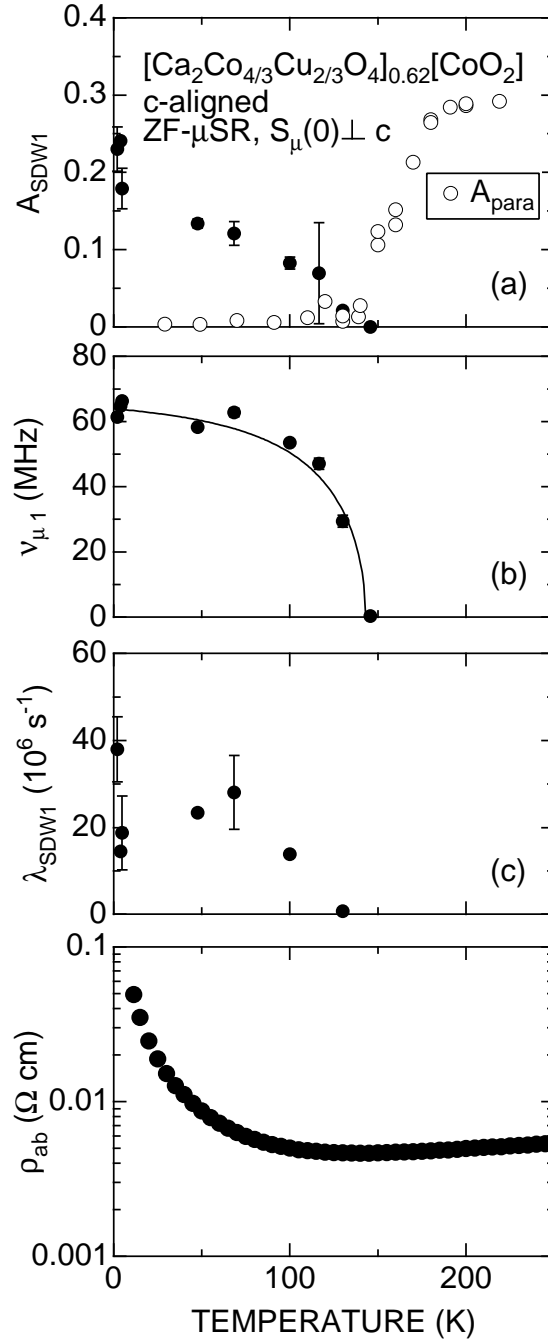


Figure 5. Temperature dependences of (a) A_{SDW1} , (b) $\nu_{\mu 1}$, (c) λ_{SDW1} , and (d) in-plane resistivity (ρ_{ab}) for the c -aligned $[\text{Ca}_2\text{Co}_{4/3}\text{Cu}_{2/3}\text{O}_4]_{0.62}^{\text{RS}}[\text{CoO}_2]$. In Figure 5(a), A_{para} obtained by the wTF- μ^+ SR experiment is also shown for comparison. The solid line in Figure 5(b) represents the temperature dependence of the BCS gap energy.

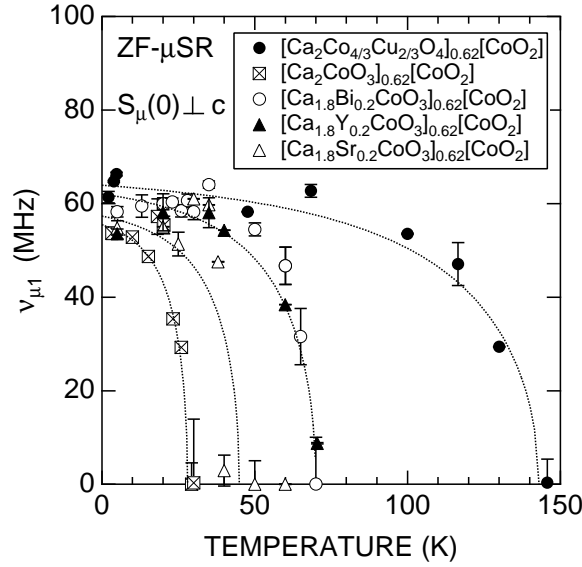


Figure 6. Temperature dependences of $\nu_{\mu 1}$ for the c -aligned $[\text{Ca}_2\text{Co}_{4/3}\text{Cu}_{2/3}\text{O}_4]_{0.62}^{\text{RS}}[\text{CoO}_2]$ and c -aligned pure and doped $[\text{Ca}_2\text{CoO}_3]_{0.62}^{\text{RS}}[\text{CoO}_2]$. The dotted lines represent the temperature dependence of the BCS gap energy.

of the cations and oxygen ion, and magnetic anisotropy. Indeed, the $\chi(T)$ curve for the $[\text{Ca}_2\text{CoO}_3]_{0.62}^{\text{RS}}[\text{CoO}_2]$ single crystals exhibited a clear but small maximum at 27 K indicating the formation of the IC-SDW order only when $H \parallel c$ [13], whereas those for the c -aligned and random polycrystalline samples did not. Therefore, if a large single crystal of $[\text{Ca}_2\text{Co}_{4/3}\text{Cu}_{2/3}\text{O}_4]_{0.62}^{\text{RS}}[\text{CoO}_2]$ is available, its $\chi_c(T)$ curve would also have an anomaly around 140 K.

The $\nu_{\mu 1}(T)$ curve is well explained by the energy gap function in the BCS weak-coupling theory (see Figure 5(b)), as expected for the IC-SDW state [20]. As seen in Figure 5(c), $\lambda_{\text{SDW}1}$ seems to increase monotonically with decreasing T . The exponential damping of the IC-SDW oscillation is most likely to be caused by the misfit between the $[\text{Ca}_2\text{Co}_{4/3}\text{Cu}_{2/3}\text{O}_4]$ and the $[\text{CoO}_2]$ subsystem along the b axis. Since we used the c -aligned sample for the current ZF- μ^+ SR measurements, the result obtained with $\vec{S}_{\mu}(0) \perp \mathbf{c}$ is the average information along the a and b axis. Thus, the anisotropic IC modulation in the $a - b$ plane is considered to be the origin of the broadening of the IC-SDW field distribution at the μ^+ sites.

3.2. Pure and Sr, Y and Bi doped $[\text{Ca}_2\text{CoO}_3]_{0.62}^{\text{RS}}[\text{CoO}_2]$

Similar anisotropic ZF- μ^+ SR spectra were also observed for the c -aligned $[\text{Ca}_2\text{CoO}_3]_{0.62}^{\text{RS}}[\text{CoO}_2]$ below ~ 30 K [13], and the ZF- μ^+ SR time spectra with $\vec{S}_{\mu}(0) \perp \mathbf{c}$ were well fitted using the Bessel function, $A_{\text{SDW}1}J_0(\omega_{\mu 1}t)\exp(\lambda_{\text{SDW}1})$.

Figure 6 shows the $\nu_{\mu 1}(T)$ curve for the c -aligned pure and doped $[\text{Ca}_2\text{CoO}_3]_{0.62}^{\text{RS}}[\text{CoO}_2]$ and $[\text{Ca}_2\text{Co}_{4/3}\text{Cu}_{2/3}\text{O}_4]_{0.62}^{\text{RS}}[\text{CoO}_2]$ samples. The data were obtained

Table 1. Internal magnetic field determined by μ^+ SR and the corresponding magnetic moment at the Co site in the $[\text{CoO}_2]$ plane estimated by equation (4). The values of $d_{\text{Co-O}}$ in the rocksalt-type subsystem are 0.213-0.230 nm in $[\text{Ca}_2\text{Co}_{4/3}\text{Cu}_{2/3}\text{O}_4]$ [21] and 0.179-0.228 nm in $[\text{Ca}_2\text{CoO}_3]$ [22].

cobaltite	$[\text{Ca}_2\text{Co}_{4/3}\text{Cu}_{2/3}\text{O}_4]_{0.62}^{\text{RS}}[\text{CoO}_2]$	$[\text{Ca}_2\text{CoO}_3]_{0.62}^{\text{RS}}[\text{CoO}_2]$
$\nu_{\mu,1}(0 \text{ K})$ (MHz)	63.9	55.5
H_{int} (kOe)	4.71	4.08
$d_{\text{Co-O}}$ in $[\text{CoO}_2]$ (nm)	0.184	0.197
m_{d} (μ_{B})	3.2	3.3

by fitting the ZF- μ^+ SR time spectra with $\vec{S}_{\mu}(0) \perp \mathbf{c}$ using equation (2). All the temperature dependences of $\nu_{\mu 1}$ for the c -aligned layered cobaltites are well fitted by the BCS weak-coupling theory. It should be noted that all the samples show approximately the same precession frequency at zero temperature, although the transition temperatures are different from 27 to ~ 140 K; i.e., $T_{\text{SDW}} = 27$ K for $[\text{Ca}_3\text{CoO}_3]_{0.62}^{\text{RS}}[\text{CoO}_2]$, ~ 45 K for $[\text{Ca}_{1.8}\text{Sr}_{0.2}\text{CoO}_3]_x^{\text{RS}}[\text{CoO}_2]$, ~ 80 K for $[\text{Ca}_{1.8}\text{Y}_{0.2}\text{CoO}_3]_x^{\text{RS}}[\text{CoO}_2]$ and $[\text{Ca}_{1.8}\text{Bi}_{0.2}\text{CoO}_3]_x^{\text{RS}}[\text{CoO}_2]$ and ~ 140 K for $[\text{Ca}_2\text{Co}_{4/3}\text{Cu}_{2/3}\text{O}_4]_{0.62}^{\text{RS}}[\text{CoO}_2]$. This suggests that the local magnetic field $H_{\text{int}}(0 \text{ K})$ is independent of both dopant and the number of layers in the rocksalt-type subsystem, if we assume that the muon sites are essentially the same in all these compounds. This supports the conclusion that the IC-SDW exists not in the rocksalt-type subsystem but in the $[\text{CoO}_2]$ plane and, as a result, the μ^+ sites are considered to be the vicinity of the O ions in the $[\text{CoO}_2]$ plane.

4. Discussion

4.1. IC-SDW: common to all the (good thermoelectric) cobaltites ?

Although the possible μ^+ sites are bound to the oxygen ions in the $[\text{CoO}_2]$ plane and the two inequivalent oxygen ions in the $[\text{Ca}_2\text{Co}_{4/3}\text{Cu}_{2/3}\text{O}_4]$ subsystem, the μ^+ sites are most likely to the vicinity of the O ions in the $[\text{CoO}_2]$ plane. We, therefore, calculate the dipole field at the O ions in the $[\text{CoO}_2]$ plane at first. The bond length d of Co-O in the $[\text{CoO}_2]$ plane is 0.184 nm in $[\text{Ca}_2\text{Co}_{4/3}\text{Cu}_{2/3}\text{O}_4]_{0.62}^{\text{RS}}[\text{CoO}_2]$ [21], whereas it is 0.197 nm in $[\text{Ca}_2\text{CoO}_3]_{0.62}^{\text{RS}}[\text{CoO}_2]$ [22]. A simple estimate of dipole field from one ion is given by;

$$H_{\text{int}} = \frac{m_{\text{d}}}{4\pi\mu_0 d^3}, \quad (4)$$

where m_{d} is the dipole moment of the Co ions in the IC-SDW state and μ_0 is the permeability of free space. Using the above d values and the observed H_{int} , we estimate $m_{\text{d}} = 3.2 \mu_{\text{B}}$ for $[\text{Ca}_2\text{Co}_{4/3}\text{Cu}_{2/3}\text{O}_4]_{0.62}^{\text{RS}}[\text{CoO}_2]$ and $3.3 \mu_{\text{B}}$ for $[\text{Ca}_2\text{CoO}_3]_{0.62}^{\text{RS}}[\text{CoO}_2]$ (see Table 1). If we ignore the effect of the distortion of the CoO_6 octahedra in the $[\text{CoO}_2]$ plane, the number of the nearest neighboring Co ions for the O ion is three [14]; hence, the ordered Co moment in the IC-SDW state is therefore roughly estimated as $\sim 1.1 \mu_{\text{B}}/\text{Co}$ ion for both compounds. This is in good agreement with the amplitude of

the IC-SDW estimated by the mean field theory ($\sim 0.86 \mu_B/\text{Co ion}$) [10]. Here, it should be noted that the muon locates probably ~ 0.1 nm away from the oxygen ions, and that there is no space for it in the CoO_6 octahedra in the $[\text{CoO}_2]$ plane as in the case for the high- T_c cuprates[19]. Thus, the accuracy of the above estimation is very limited; i.e., $m_d=0.3\text{-}11.7 \mu_B$ for $[\text{Ca}_2\text{Co}_{4/3}\text{Cu}_{2/3}\text{O}_4]_{0.62}^{\text{RS}}[\text{CoO}_2]$, if $d_{\text{Co}-\mu} = 0.184 \pm 0.1$ nm. In order to determine the μ^+ sites, both further experiments on the layered cobaltites and a theoretical research are necessary.

There are two Co sites in the $[\text{Ca}_2\text{Co}_{4/3}\text{Cu}_{2/3}\text{O}_4]_{0.62}^{\text{RS}}[\text{CoO}_2]$ lattice. Thus, it is difficult to determine the Co valence in the $[\text{CoO}_2]$ plane by a χ measurement or a chemical titration technique alone. Here, we assume that the magnitude of S depends on the concentration y of Co^{4+} ions in the $[\text{CoO}_2]$ plane as [23];

$$S_{T \rightarrow \infty} = -\frac{k_B}{e} \ln\left(\frac{g_3}{g_4} \frac{y}{1-y}\right), \quad (5)$$

where k_B is the Boltzmann constant, e is the elementary charge and g_3 and g_4 are the multiplying numbers of the spin configurations of Co^{3+} and Co^{4+} , respectively. Since the electron configurations of both Co^{3+} and Co^{4+} are in the low-spin state (t_{2g}^6 and t_{2g}^5) [5, 6, 10, 24, 8], $g_3=1$ and $g_4=6$. Then, using the value of $S(300 \text{ K}) \sim 150 \mu\text{VK}^{-1}$, we obtain $y \sim 0.51$, i.e. the average valence of the Co ions in the $[\text{CoO}_2]$ plane is $+3.51$. This indicates that almost the same amounts of Co^{3+} and Co^{4+} coexist in the $[\text{CoO}_2]$ plane. In other words, the Co spin ($\mathbf{S}=1/2$) occupies about half of the sites of the two-dimensional-triangular lattice of Co ions. This is significant to achieve the IC-SDW long-range order in the triangular lattice. In addition, the average Co moment is calculated as $\sim 0.86 \mu_B/\text{Co ion}$, which is consistent with the value estimated above.

It is worth noting that μ^+ sites are bound to the O ions in the $[\text{CoO}_2]$ plane. This means that the μ^+ feel mainly the magnetic field in the $[\text{CoO}_2]$ plane. Thus, the IC-SDW is most unlikely to be caused by the misfit between the two subsystems, but to be an intrinsic behavior of the $[\text{CoO}_2]$ plane. Indeed, the recent $\mu^+\text{SR}$ experiments on $[\text{Na}]_x[\text{CoO}_2]$, which consist of the alternating stack of Na and $[\text{CoO}_2]$ planes, also indicate the existence of a commensurate SDW or a ferrimagnetic state below 22 K for $[\text{Na}]_{0.75}[\text{CoO}_2]$ [25] and an IC-SDW state below 19 K for $[\text{Na}]_{0.9}[\text{CoO}_2]$ [26]. Therefore, it is concluded that the IC-SDW state is a common behavior for the layered cobaltites, although the magnitude of T_{SDW} depends on the Co valence in the $[\text{CoO}_2]$ plane and the structure of the subsystem sandwiched by the two $[\text{CoO}_2]$ planes (see Figure 6).

The IC-SDW order in the two layered cobaltites is assigned to be a spin ($\mathbf{S}=1/2$) order on the two-dimensional triangular lattice (i.e. the CoO_2 plane) at non-half filling. Such a problem was investigated by several workers using the Hubbard model within a mean field approximation [28, 29, 30];

$$\mathcal{H} = -t \sum_{\langle ij \rangle \sigma} c_{i\sigma}^\dagger c_{j\sigma} + U \sum_i n_{i\uparrow} n_{i\downarrow}, \quad (6)$$

where $c_{i\sigma}^\dagger (c_{j\sigma})$ creates (destroys) an electron with spin σ on site i , $n_{i\sigma} = c_{i\sigma}^\dagger c_{i\sigma}$ is the number operator, t is the nearest-neighbor hopping amplitude and U is the Hubbard

on-site repulsion. The electron filling n is defined as $n = (1/2N)\sum_i^N n_i$, where N is the total number of sites.

At $T=0$ and $n=0.5$ (i.e., the average valence of the Co ions in the $[\text{CoO}_2]$ plane is $+4$), as U increased from 0, the system is paramagnetic metal up to $U/t \sim 3.97$, and changes into a metal with a spiral IC-SDW, and then at $U/t \sim 5.27$, a first-order metal-insulator transition occurs [28]. Also the calculations predict that [29, 30], as n increases from 0, the magnitude of U/t at the boundary between the paramagnetic and SDW phases decreases with increasing slope ($d(U/t)/dn$) up to $n=0.75$. Even for $U/t=0$, the SDW phase is stable at $n=0.75$. U/t increases with further increasing n , with decreasing slope. In other words, at $n=0.75$ (i.e. the average valence of the Co ions in the $[\text{CoO}_2]$ plane is $+3.5$), a spiral IC-SDW state is expected to appear at the highest temperature in the n range between 0.5 and 1 [29].

The value of n is estimated as 0.74 for $[\text{Ca}_2\text{Co}_{4/3}\text{Cu}_{2/3}\text{O}_4]_{0.62}^{\text{RS}}[\text{CoO}_2]$ and 0.715, 0.70, 0.73 and 0.73 for pure, Sr-, Y-, and Bi-doped $[\text{Ca}_2\text{CoO}_3]_{0.62}^{\text{RS}}[\text{CoO}_2]$ respectively, using eq. (5) and $S(300 \text{ K})$. Therefore, the fact that T_{SDW} for $[\text{Ca}_2\text{Co}_{4/3}\text{Cu}_{2/3}\text{O}_4]_{0.62}^{\text{RS}}[\text{CoO}_2]$ is higher than those for pure and doped $[\text{Ca}_2\text{CoO}_3]_{0.62}^{\text{RS}}[\text{CoO}_2]$ (see Figure 6) is roughly explained by the model calculations, if we ignore the data for Sr-doped $[\text{Ca}_2\text{CoO}_3]_{0.62}^{\text{RS}}[\text{CoO}_2]$.

Also, it should be pointed out that the increased two-dimensionality induced by the increase in the interlayer distance between CoO_2 planes plays a significant role to increase T_{SDW} . This is because T_{SDW} for $[\text{Ca}_2\text{Co}_{4/3}\text{Cu}_{2/3}\text{O}_4]_{0.62}^{\text{RS}}[\text{CoO}_2]$ is considerably higher than those for pure and doped $[\text{Ca}_2\text{CoO}_3]_{0.62}^{\text{RS}}[\text{CoO}_2]$. Here, we repeat the prediction of the model calculations. That is, the SDW phase is stable at $n=0.75$ even for $U/t=0$; this means that, on the ideal two-dimensional triangular lattice at $n=0.75$, the SDW spin structure appears at temperatures below its melting point. Indeed, the large observed transition width (60 K) are consistent with enhanced two-dimensionality and resulting spin fluctuations. Therefore, not only the shift of n towards the optimal value (0.75) but also the enhanced two-dimensionality are considered to increase T_{SDW} for $[\text{Ca}_2\text{Co}_{4/3}\text{Cu}_{2/3}\text{O}_4]_{0.62}^{\text{RS}}[\text{CoO}_2]$.

Since the magnitude of $\nu_{\mu 1}$ indicates the amplitude of the IC-SDW directly, there are two predominant factors for $\nu_{\mu 1}$. That is, the magnitude and direction of the Co spin in the $[\text{CoO}_2]$ plane. The former is a constant at low temperatures, because the spin configurations for Co^{3+} and Co^{4+} ions ($\mathbf{S}=0$ and $1/2$) are not affected by both dopant and the number of layers in the rocksalt-type subsystem. The latter is a function of magnetic anisotropy in the lattice. Here the magnetic anisotropy in $[\text{Ca}_2\text{Co}_{4/3}\text{Cu}_{2/3}\text{O}_4]_{0.62}^{\text{RS}}[\text{CoO}_2]$ is most likely to be equivalent to that in $[\text{Ca}_2\text{CoO}_3]_{0.62}^{\text{RS}}[\text{CoO}_2]$ due to similar environment around the $[\text{CoO}_2]$ plane in the two cobaltites. That is, the first and second nearest adjacent plane for the $[\text{CoO}_2]$ plane are the Ca-O and $(\text{Co}_{2/3}\text{Cu}_{1/3})\text{-O}$ or Co-O plane in the rocksalt-type subsystem, although the third nearest plane is different for the two cobaltites. Therefore, $\nu_{\mu 1}(0 \text{ K})$ is considered to be approximately same for all the cobaltites investigated here (see Fig. 6).

4.2. The anomaly at ~ 85 K in the susceptibility

The $\chi(T)$ curve exhibits a clear anomaly at ~ 85 K, while the results of both wTF- μ^+ SR and ZF- μ^+ SR do not (see Figures 2, 4 and 5). On the other hand, there is no marked anomaly at 140 - 200 K in the $\chi(T)$ curve (see Figure 1), although μ^+ SR detects the formation of the IC-SDW state. This is quite similar to the case for $[\text{Ca}_2\text{CoO}_3]_{0.62}^{\text{RS}}[\text{CoO}_2]$; where according to the μ^+ SR experiments, it was found that the short-range IC-SDW order appeared below ~ 100 K and the long-range order completed below 27 K, whereas the $\chi(T)$ curve below 300 K only exhibited a ferrimagnetic transition at 19 K [10, 11, 12, 13].

The structures of the IC-SDW of both compounds are considered to be essentially the same, as discussed above. For $[\text{Ca}_2\text{CoO}_3]_{0.62}^{\text{RS}}[\text{CoO}_2]$, the IC-SDW is induced by ordering of the Co moments in the $[\text{CoO}_2]$ plane, whereas the ferrimagnetic ordering arises because of the interlayer coupling between the Co spins in the $[\text{CoO}_2]$ and $[\text{Ca}_2\text{CoO}_3]$ subsystems [12, 13].

As seen in Figure 5(b), the microscopic internal IC-SDW field does not change around 85 K. Furthermore, the extremely small value of the asymmetry of the exponential relaxation function A_F , even at 2.1 K, (see Figure 5(a)) suggests that the anomaly at ~ 85 K is not a transition to a spin-glass state [18, 19, 27]. Therefore, the anomaly at ~ 85 K is most likely caused by some order between the two subsystems, i.e., the $[\text{Ca}_2\text{Co}_{4/3}\text{Cu}_{2/3}\text{O}_4]$ and the $[\text{CoO}_2]$. The interlayer coupling between both subsystems is expected to be basically antiferromagnetic (AF), because there was no clear $M - H$ loop even at 5 K. In other words, a two-dimensional AF (IC-SDW) order of the Co spins completes at 140 K, whereas a three-dimensional AF order occurs below ~ 85 K.

The $[\text{Ca}_2\text{Co}_{4/3}\text{Cu}_{2/3}\text{O}_4]$ subsystem consists of two Ca-O planes and two $(\text{Co}_{2/3}\text{Cu}_{1/3})\text{-O}$ planes; so that, the two $(\text{Co}_{2/3}\text{Cu}_{1/3})\text{-O}$ planes are sandwiched by the two Ca-O planes. Considering the fact that 1/3 of the Co ions are replaced by Cu ions and that the thickness of the rocksalt-type subsystem increases due to the extra $(\text{Co}_{2/3}\text{Cu}_{1/3})\text{-O}$ plane, the coupling along the c -axis for $[\text{Ca}_2\text{Co}_{4/3}\text{Cu}_{2/3}\text{O}_4]_{0.62}^{\text{RS}}[\text{CoO}_2]$ is rather weak compared with that for $[\text{Ca}_2\text{CoO}_3]_{0.62}^{\text{RS}}[\text{CoO}_2]$. This weak coupling is likely to be a significant factor for the thermal hysteresis of the $\chi(T)$ curve. That is, the IC-SDW in each $[\text{CoO}_2]$ plane is considered to be moved by the external magnetic field (~ 10 kOe) at 85 - 140 K, but fixed below ~ 85 K.

5. Summary

In order to elucidate the magnetism in 'good' thermoelectric layered cobaltites, μ^+ SR spectroscopy has been used on a c -aligned polycrystalline $[\text{Ca}_2\text{Co}_{4/3}\text{Cu}_{2/3}\text{O}_4]_{0.62}^{\text{RS}}[\text{CoO}_2]$ sample at temperatures below 300 K. It was found that $[\text{Ca}_2\text{Co}_{4/3}\text{Cu}_{2/3}\text{O}_4]_{0.62}^{\text{RS}}[\text{CoO}_2]$ exhibits a transition at around 140 K from a paramagnetic to an incommensurate spin density wave IC-SDW state, although a short-range order appears below ~ 180 K.

By comparison with the μ^+ SR results on pure and doped $[\text{Ca}_2\text{CoO}_3]_{0.62}^{\text{RS}}[\text{CoO}_2]$, the IC-SDW appears to be common behavior for these cobaltites. The characteristic features of the IC-SDW are as follows;

- (i) A long-range IC-SDW order completes below T_{SDW} , while a short-range order is observed at 40 - 60 K higher than T_{SDW} with a transition width $\Delta T = 40 - 60$ K.
- (ii) The IC-SDW propagates in the a - b plane, with oscillating moments directed along the c axis.
- (iii) The IC-SDW exists not in the rocksalt-type subsystem but in the $[\text{CoO}_2]$ plane.

The magnitude of T_{SDW} is found to be sensitive both to the Co valence in the $[\text{CoO}_2]$ plane, i.e., the occupancy of the Co spin ($S=1/2$) in the triangular lattice, and to the structure of the subsystem sandwiched by the two $[\text{CoO}_2]$ planes. Therefore, physical properties of the layered cobaltites should be investigated systematically as functions of the Co valence in the $[\text{CoO}_2]$ plane and the distance between the two adjacent $[\text{CoO}_2]$ planes.

Acknowledgments

We thank Dr. S.R. Kreitzman and Dr. D.J. Arseneau of TRIUMF for help with the μ^+ SR experiments. Also, we thank Mr. A. Izadi-Najafabadi and Mr. S.D. LaRoy of University of British Columbia for help with the experiments. We appreciate useful discussions with Dr. R. Asahi of Toyota CRDL, Professor U. Mizutani, Professor H. Ikuta and Professor T. Takeuchi of Nagoya University. This work was supported at Toyota CRDL by joint research and development with International Center for Environmental Technology Transfer in 2002-2004, commissioned by the Ministry of Economy Trade and Industry of Japan, at UBC by the Canadian Institute for Advanced Research, the Natural Sciences and Engineering Research Council of Canada, and at TRIUMF by the National Research Council of Canada.

References

- [1] Molenda J, Delmas C, Dordor P and Stoklosa A 1989 *Solid State Ionics* **12** 473
- [2] Yakabe H, Kikuchi K, Terasaki I, Sasago Y and Uchinokura K 1997 *Proc. 16th Int. Conf. on Thermoelectrics (Dresden)* (Piscataway: Institute of Electrical and Electronics Engineers, Inc.) pp 523-527
- [3] Terasaki I, Sasago Y and Uchinokura K 1997 *Phys. Rev. B* **56** R12685
- [4] Funahashi R, Matsubara I, Ikuta H, Takeuchi T, Mizutani U and Sodeoka S 2000 *Jpn. J. Appl. Phys.* **39** L1127
- [5] Masset A C, Michel C, Maignan A, Hervieu M, Toulemonde O, Studer F, Raveau B and Hejtmanek J 2000 *Phys. Rev. B* **62** 166
- [6] Miyazaki Y, Kudo K, Akoshima M, Ono Y, Koike Y and Kajitani T 2000 *Jpn. J. Appl. Phys.* **39** L531
- [7] Tsukada I, Yamamoto T, Takagi M, Tsubone T, Konno S and Uchinokura K 2001 *J. Phys. Soc. Jpn.* **70** 834
- [8] Yamamoto T, Uchinokura K and Tsukada I 2002 *Phys. Rev. B* **65** 184434

- [9] Fujii T, Terasaki I, Watanabe T and Matsuda A 2002 *Jpn. J. Appl. Phys.* **41** L783
- [10] Sugiyama J, Itahara H, Tani T, Brewer J H and Ansaldo E J 2002 *Phys. Rev. B* **66** 134413
- [11] Sugiyama J, Brewer J H, Ansaldo E J, Bayer M, Itahara H and Tani T 2003 *Physica B* **326** 518
- [12] Sugiyama J, Brewer J H, Ansaldo E J, Itahara H, Seno Y, Dohmae K, Xia C and Tani T 2003 *Phys. Rev. B* in press
- [13] Sugiyama J, Xia C and Tani T 2003 *Phys. Rev. B* **67** 104410
- [14] Miyazaki Y, Miura T, Ono Y and Kajitani T 2002 *Jpn. J. Appl. Phys.* **41** L849
- [15] Tani T, Itahara H, Xia C and Sugiyama J 2003 *J. Mater. Chem.* **13** 1865
- [16] Itahara H *et al.* 2003 unpublished
- [17] Le L P, Keren A, Luke G M, Sternlieb B J, Wu W D, Uemura Y J, Brewer J H, Riseman T M, Upasani R V, Chiang L Y, Kang W, Chaikin P M, Csiba T and Grüner G 1993 *Phys. Rev. B* **48** 7284
- [18] Uemura Y J 1999 *Muon Science* (Bristol: Institute of Physics Publishing) pp 85-114 and references cited therein
- [19] Kalvius G M, Noakes D R and Hartmann O 2001 *Handbook on the Physics and Chemistry of Rare Earths* vol 32 (Amsterdam: North-Holland) pp 55-451 and references cited therein
- [20] Grüner G 1994 *Density Waves in Solids* (Reading: Addison-Wesley-Longmans) pp 71-85 and references cited therein
- [21] Miyazaki Y *et al.* 2003 unpublished
- [22] Miyazaki Y, Onoda M, Oku T, Kikuchi M, Ishii Y, Ono Y, Morii Y and Kajitani T 2002 *J. Phys. Soc. Jpn.* **71** 491
- [23] Koshibae W, Tsutsui K and Maekawa S 2000 *Phys. Rev. B* **62** 6869
- [24] Hébert S, Lambert S, Pelloquin D and Maignan A 2001 *Phys. Rev. B* **64** 172101
- [25] Sugiyama J, Itahara H, Brewer J H, Ansaldo E J, Motohashi T, Karppinen M and Yamauchi H 2003 *Phys. Rev. B* **67** 214420
- [26] Sugiyama J *et al.* 2003 unpublished
- [27] Campbell I A 1999 *Muon Science* (Bristol: Institute of Physics Publishing) pp 137-148 and references cited therein
- [28] Krishnamurthy H R, Jayaprakash C, Sarker S and Wenzel W 1990 *Phys. Rev. Lett.* **64** 950
- [29] Fujita M, Ichimura M and Nakao K 1991 *J. Phys. Soc. Jpn.* **60** 2831
- [30] Fujita M, Nakanishi T and Machida K 1992 *Phys. Rev. B* **45** 2190